RSC Advances

ROYAL SOCIETY OF CHEMISTRY

www.rsc.org/advances

RSC Advances

COMMUNICATION

Preparation of hierarchical flower-like γ-Al_2O_3@C composite exhibiting enhanced adsorption performance for Congo Red by high temperature transformation of γ-AlOOH@C precursors

Received 00th January 20xx,
Accepted 00th January 20xx

DOI: 10.1039/x0xx00000x

www.rsc.org/

Beibei Fang, Zepei Bao, Lun Lu, Lijun Zhao*, Huiyuan Wang*

Hierarchical flower-like γ-Al_2O_3@C composite was synthesized via a hydrothermal method combined with a heat treatment process using glucose and Al nanopowders as reactants. Herein, glucose plays key roles in the formation of flower-like structure and carbon shell. Due to high specific surface area of flower-like γ-Al_2O_3@C composite (346.2 $m^2 \cdot g^{-1}$), its adsorption ability was investigated. Organic dye Congo red (CR) was selected as a subject in the study. Over 90% of CR could be removed from aqueous solution within 5 min, and the final adsorption capacity reaches 244.5 $mg \cdot g^{-1}$ which is much higher than most of γ-AlOOH and γ-Al_2O_3 materials reported before, indicating it would be a promising material used in the water treatment industry.

Nowadays, water pollution is one of the biggest and the most alarming problems that demands formidable and effective solutions.[1, 2] Congo red (CR), which is well known as a carcinogenic azo dye pollution source.[3] The treatment of CR in wastewater is difficult, because the dye is generally present in sodium salt form giving it very good water solubility. So far, adsorption technique is widely regarded as a promising method for removing hazardous and environmentally undesirable chemicals such as azo dyes.[4] Some nano-adsorbents such as carbons, metal oxides, transition metal oxides, and composites etc. have been used for the removal of CR from aqueous solutions.[5-8] However, simple preparation method, low-cost and nontoxic raw materials, and good adsorption efficiency are still challenges for using the above-mentioned nanostructures.

Combining multiple components into one material is useful for sewage treatment. [9-11] To overcome low adsorption efficiency, toxic, and complex preparation procedures of the current adsorbents, it would be very meaningful to design a composite consisting of common materials, such as alumina and carbon. In previous reports, both alumina and carbon are the most frequently used as water treatment material.[12, 13] Although lots of alumina and carbon materials have been applied in water treatment, as far as we know, there is rare report about the investigation on CR removal and adsorption mechanism using composite of alumina and carbon.

Herein, hierarchical flower-like γ-Al_2O_3@C composite was synthesized via a hydrothermal method combined with a heat treatment process using glucose and Al nanopowders as reactants (detailed experimental methods and characterizations seen in ESI). Significantly, the hierarchical flower-like γ-Al_2O_3@C composite showed high specific surface area and exhibited excellent efficient absorption ability for CR.

A typical X-ray diffraction (XRD) pattern of the γ-Al_2O_3@C composite is shown in Figure 1a, and the two wide angle diffraction peaks can be perfectly indexed to the cubic γ-Al_2O_3 (JCPDS card No. 10-0425). However, no obvious diffraction signals of C phase have been detected, which might be attributed to thin carbon layer and amorphous structure. Compared the XRD pattern of γ-Al_2O_3@C composite with the XRD pattern of corresponding precursor (seen in Figure S1, ESI), it can be found that γ-AlOOH is completely transformed to γ-Al_2O_3 after calcinations. SEM and TEM images of the flower-like γ-Al_2O_3@C composite are shown in Figure 1b to 1d. Compared with the SEM and TEM images of corresponding precursor (seen in Figure S2, ESI), it can be observed that the morphology of γ-Al_2O_3@C composite still presents the uniform and well-distributed hierarchical flower-like structures even after 600 °C of calcinations, and the thickness of nanoflakes is about 3 nm

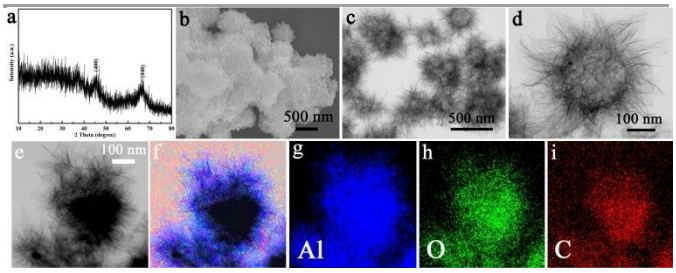

Figure 1 Flower-like γ-Al_2O_3@C composite: (a) XRD pattern; (b) SEM image; (c, d) TEM images with different magnifications; (e) STEM images; (f) mixed elemental mappings image; corresponding elemental mappings for (g) Al, (h) O, and (i) C

Key Laboratory of Automobile Materials (Jilin University), Ministry of Education and School of Materials Science and Engineering, Jilin University, Changchun 130022, China Fax: +86-0431-85095876
E-mail: lijunzhao@jlu.edu.cn, wanghuiyuan@jlu.edu.
Electronic Supplementary Information (ESI) available: [details of any supplementary information available should be included here]. See DOI: 10.1039/x0xx00000x

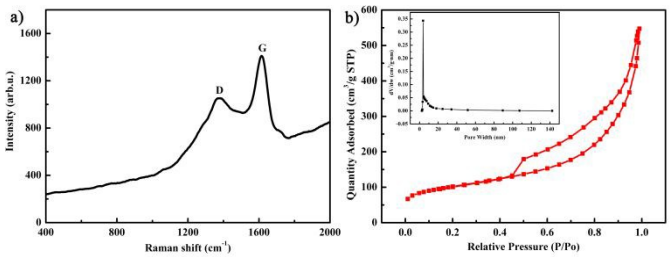

Figure 2 (a) Raman spectra and (b) Nitrogen adsorption/desorption isotherm and corresponding Barrett-Joyner-Halenda (BJH) pore size distribution plot (inset) of flower-like γ-Al_2O_3@C composite

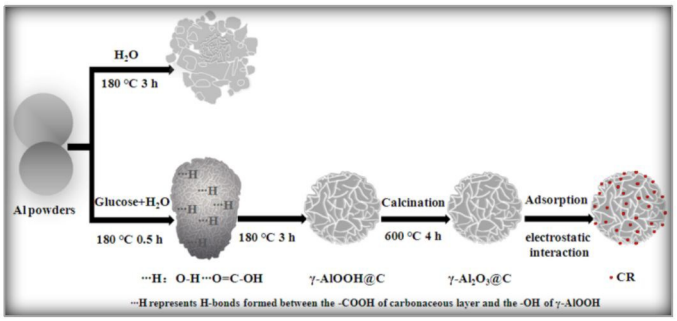

Scheme 1 Formation process of flower-like γ-Al_2O_3@C composite and CR adsorption diagram

measured from SEM image. The size distribution from the TEM image exhibits that the particles are in the size range of 280-480 nm, and the average size is about 360 nm. The size and morphology of γ-Al_2O_3@C composite are extremely similar to those of the γ-AlOOH@C precursor, indicating that the size and morphology can be well preserved by carbon during the phase-transformation. From STEM image in Figure 1e and the corresponding elemental mappings in Figure 1f to 1i, Al, O and C atoms are uniformly distributed in the whole particle, which further indicates that flower-like γ-Al_2O_3@C composite is synthesized.

Raman spectroscopy was used to further characterize the presence of carbon coating on the surface of γ-Al_2O_3@C composite, and the result is shown in Figure 2a. The peak at about 1600 cm^{-1} (G band) corresponds to the vibration of sp^2-bonded carbon atoms, and the D band at about 1370 cm^{-1} is ascribed to defects like edges and disordered carbon.[14] The calculated I_D/I_G ratio is around 0.76, indicating the predominantly amorphous/disordered carbon nature, which is totally consistent of the XRD results and further proves the existence of carbon coating. To investigate the specific surface area and porosity of the as-prepared γ-Al_2O_3@C composite, N_2 adsorption analysis was carried out. As shown in Figure 2b, the isotherm of the sample is type IV, which is characteristic of mesoporous materials.[15] The BET surface area was calculated to be 346.2 $m^2 g^{-1}$, showing that the sample has a relatively high surface-to-volume ratio. The corresponding BJH pore size distribution plot is shown in the inset of Figure 2b, which reveals a quite narrow distribution for the γ-Al_2O_3@C composite centered at 3-4 nm. Furthermore, the pore volume is estimated to be 0.68 $cm^3 \cdot g^{-1}$. The flower-like γ-Al_2O_3@C composite possesses extremely high BET surface area and large pore volume which may be due to its nanoflakes-aggregated structure.

To investigate the role of glucose, γ-AlOOH product was prepared in the absence of glucose. Only lamellar structures were formed (seen in Figure S3 and S4, ESI). It is reasonable to consider that glucose is a very important factor on the growth process of the flower-like γ-Al_2O_3@C, not only as carbon resources but also deciding the formation of flower-like morphology. To obtain the proper flower-like γ-AlOOH@C composite, the best reaction temperatures and time were investigated (Figure S5 and S6, ESI). The well-defined γ-AlOOH@C precursor can be obtained at 180 °C for 3 h. During the hydrothermal process at 180 °C, Al powders reacted with H_2O, then $Al(OH)_3$ was present. Because the newly formed $Al(OH)_3$ was active and unstable, it further dehydrated and converted to γ-AlOOH. After 0.5 h of hydrothermal treatment, the surface of Al microsphere became coarse and small γ-AlOOH nanoflakes were formed. Meanwhile, amorphous carbonaceous layer with large number of oxygen-containing functional groups uniformly covered on the surface of γ-AlOOH nanoflakes due to the dehydration and aromatization of glucose.[16,17] Hydrogen bonds were formed between the carboxyl of carbonaceous layer and the hydroxyl ions in adjacent planes of AlO_6 octahedral of γ-AlOOH, which restrained the further nucleation and growth of these new formed nanoflakes to large area of lamellar structures.[18, 19] With the increasing of carbonaceous amount coated on the surface of γ-AlOOH nanoflakes, which favors the self-assembly of nanoflakes by van der Waals forces and the hydrogen bonding into 3D architectures.[20] Since the raw Al powders have a certain degree of aggregation, large sized ellipsoidal and subsphaeroidal γ-AlOOH@C assemblies were obtained. (Figure S6a, ESI). An increase of the reaction time initiated the epitaxial growth of the newly formed nanoflakes and the further dissolution process of those ellipsoidal and subsphaeroidal structures to achieve a minimum total surface free energy,[21] and thus uniformly distributed flower-like γ-AlOOH@C composite with thicker carbon coating were fabricated. Finally, the γ-AlOOH@C precursor was calcined at 600 °C to achieve the topotactic phase transition from flower-like γ-AlOOH to flower-like γ-Al_2O_3@C composite. The above-mentioned process was exhibited in scheme 1. When there was no glucose participating in the hydrothermal process, without the function of hydrogen bonds, the γ-AlOOH crystallites prefer to grow on the edges of the already existing nanoflakes along the main crystallographic [001] axis to form nanoflakes with higher thermodynamic stability under appropriate basic hydrothermal conditions. [15] Thus, a large area of lamellar γ-AlOOH was formed (seen in Figure S4, ESI). From the above discussions, it is noting that glucose is not only as carbon source, but also controls the formation of flower-like structure. The flower-like structure for the γ-Al_2O_3@C composite have given it the high BET surface area and large pore volume which make it a promising candidate for application in dyes removal from water.

TG/DTA analyses of γ-AlOOH were performed under Ar atmosphere to investigate the transformation of γ-AlOOH to γ-Al_2O_3 (Figure S7, ESI). It can be found that the weight loss occurred in three steps with a total weight loss of approximately 44.2%. The three endothermic DTA peaks of the first stage (below 120 ℃) were caused by desorption of physically adsorbed water, and it corresponded to 17% of weight loss. The second stage ranged from

RSC Advances

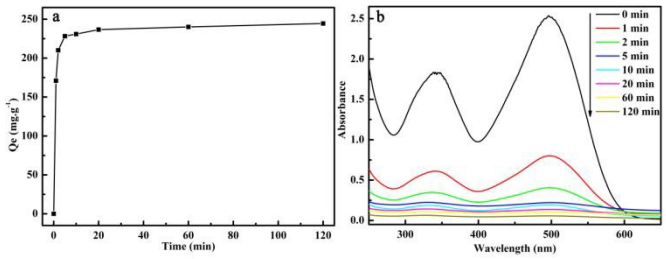

Figure 3 (a) Time-dependent CR adsorption capacities on γ-Al_2O_3@C and (b) corresponding successive UV-visible spectra of CR adsorption at different time intervals.

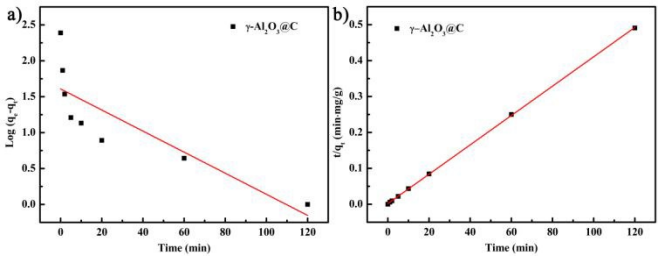

Figure 4 Pseudo-first-order kinetics (a) and pseudo-second-order kinetics (b) for the adsorption of CR on γ-Al_2O_3@C.

120~400 ℃, and the TG curve shows a continuous weight loss of 13.9% due to the evaporation of residual water. At even higher temperatures (400~600 ℃), the strong endothermic DTA peak around 450 ℃ can be contributed to the dehydroxylation of γ-AlOOH and its transformation into γ-Al_2O_3, and the corresponding weight loss is 13.3%.

To further confirm the flower-like γ-Al_2O_3@C composite possessing good adsorption abilities, the CR adsorption experiment was carried out at room temperature (Adsorption Experiments for CR seen in ESI). Figure 3a shows the calculated adsorption capacity of the γ-Al_2O_3@C which possesses high adsorption rate. Over 90% of CR can be removed from aqueous solution within 5 min. With the prolonging of adsorption time, the final adsorption capacity of the γ-Al_2O_3@C can reach as high as 244.5 mg·g^{-1}. Results show that the as-prepared γ-Al_2O_3@C powders exhibit excellent adsorption efficiency than most of γ-AlOOH and γ-Al_2O_3 materials reported before (Table S1, ESI). From the corresponding successive UV-visible spectra (Figure 3b), the quick decrease of the CR concentration can also be visually observe. Furthermore, the γ-Al_2O_3@C samples containing CR could be regenerated by a simple thermal treatment under Ar atmosphere at 280 °C for 4 h, [22]and the results are shown in Figure S8, ESI. It can be found that their performance kept quiet well after the first regeneration (curves b). With the increase of cycle index, though the adsorption performance weakly decreased, the final removal ability of the regenerated material after four cycles can kept 92.8% of the original.

For comparison, the adsorption experiments of pure γ-Al_2O_3 (the corresponding XRD pattern is shown in Figure S11, ESI) and pure carbon sample for CR were also performed, as shown in Figure S9, ESI. Their adsorption capacities and adsorption rate were listed in Table S2, ESI. It's obvious that the γ-Al_2O_3@C composite exhibits much better adsorption efficiency than the other two samples.

N_2 adsorption analysis of pure γ-Al_2O_3 and carbon samples was also carried out (Figure S10, ESI). The surface areas of γ-Al_2O_3 and carbon were calculated to be 282.2 $m^2 \cdot g^{-1}$ and 426.5 $m^2 \cdot g^{-1}$, respectively (Table S3, ESI). The pore volume of γ-Al_2O_3 and carbon were separately estimated to be 1.16 $cm^3 \cdot g^{-1}$ and 0.25 $cm^3 \cdot g^{-1}$. Compared with the values of γ-Al_2O_3@C composite, though the carbon sample possessed the highest surface area, it still displayed far lower adsorption performance than those of the other two samples due to its quiet low pore volume and almost negligible mesoporous. The γ-Al_2O_3 has larger pore volume while lower BET surface area than those of γ-Al_2O_3@C, so its adsorption capacities are lower than γ-Al2O3@C. In general, the remarkable adsorption ability of γ-Al_2O_3@C can be contributed to the combined effect of high specific surface area, large pore volume and narrowpore sizedistribution centered at 3-4 nm.

Table 1 Adsorption parameters got from the two kinetic models for the adsorption of CR on γ-Al_2O_3@C.

kinetic models	q_e (mg·g^{-1})	k	R_2
pseudo-first-order	40.7	3.36×10^{-2} (min^{-1})	0.6614
pseudo-second-order	244.49	9.14×10^{-3} (g·mg^{-1} min^{-1})	0.9999 2

The kinetic curves of the CR adsorption on γ-Al_2O_3@C were investigated using different kinetic models, and pseudo-first-order (eq 1) and pseudo-second-order (eq 2) are given below.

Pseudo first order: $$log(q_e - q_t) = \log q_e - \frac{k_1}{2.303} t \quad \text{eq 1}$$

Pseudo second order: $$\frac{t}{q_t} = \frac{1}{k_2 q_e^2} + \frac{1}{q_e} t \quad \text{eq 2}$$

In the above equations, the corresponding rate constants are denoted by k_1 (min^{-1}) and k_2 (g·mg^{-1} min^{-1}), and q_e and q_t indicate the amount of CR adsorbed (mg·g^{-1}) at equilibrium and at time t, respectively.

Figure 4 shows the two time-dependent plots, and the corresponding calculated kinetic parameters are listed in Table 1. The comparison of correlation coefficients (R^2) of both models suggests that the adsorption mechanism of γ-Al_2O_3@C can be better explained by pseudo-second-order (0.99992) than pseudo-first-order (0.6614). Furthermore, the calculated adsorption capacity 244.49 mg·g^{-1} from the pseudo-second-order kinetics is extremely consistent with the experimental adsorption capacity 244.5 mg·g^{-1}. However, the calculated adsorption capacity 40.7 mg·g^{-1} from the pseudo-first-order is much smaller than the experimental value. All these above data shows that the adsorption process present an ideal fit to the pseudo-second-order kinetics, indicating the adsorption mechanism depends on the adsorbate and adsorbent.

Based on the adsorption kinetics and experimental results, the main adsorption mechanism may be explained as electrostatic interaction (scheme 1). CR molecules possess sulfonic acid group and amine group (–NH_2) which can be completely dissolved and protonated in water, thus become negative charged and positive charged in water, respectively.[23] The carbon coating with negative

charges[24,25] of γ-Al_2O_3@C composites are prone to adsorb the protonated and positively charged –NH_2, accordingly the CR adsorbed on the surface of composites. At last, the clear solution was obtained after the electrostatic interaction between the γ-Al_2O_3@C and CR.

Conclusions

In summary, hierarchical flower-like γ-Al_2O_3@C composite was successfully synthesized by a facile and environmentally friendly one-step hydrothermal route followed by a heat treatment process. During the reaction system, glucose not only as carbon source, but also controlled the formation of the flower-like products. Moreover, a possible glucose promoted formation mechanism was proposed. Further adsorption investigation indicates that the as-obtained γ-Al_2O_3@C composite possesses high adsorption efficiency for CR removal in aqueous solutions, and the adsorption capacity can be as high as 244.5 $mg \cdot g^{-1}$ which is much higher than most of γ-AlOOH and γ-Al_2O_3 materials reported before. Hence, the novel hierarchical flower-like γ-Al_2O_3@C composite may be a promising material for dyes sewage treatment.

Acknowledgements

This work was financially supported by the National Natural Science Foundation of China (Grant No.51501068) and 2013 Open Foundation of the Key Lab of Automobile Materials, Jilin University, from Natural Scientific Basic Research Fund for Platform and Base Construction (Grant No. 13-450060491571)

Notes and references

1. S. K. Kansal and A. Kumari, *Chem Rev*, 2014, **114**, 4993-5010.
2. R. K. Upadhyay, N. Soin and S. S. Roy, *RSC Adv.*, 2014, **4**, 3823-3851.
3. I. Ali, *Chem Rev*, 2012, **112**, 5073-5091.
4. Y. X. Zhang, X. Y. Yu, Z. Jin, Y. Jia, W. H. Xu, T. Luo, B. J. Zhu, J. H. Liu and X. J. Huang, *J Mater Chem*, 2011, **21**, 16550-16557.
5. R. Ahmad and R. Kumar, *Applied Surface Science*, 2010, **257**, 1628-1633.
6. W. Cai, Y. Hu, J. Chen, G. Zhang and T. Xia, *CrystEngComm*, 2012, **14**, 972-977.
7. J. Wu, J. Wang, H. Li, Y. Du, K. Huang and B. Liu, *Journal of Materials Chemistry A*, 2013, **1**, 9837.
8. X. Li, S. Xiong, J. Li, J. Bai and Y. Qian, *J Mater Chem*, 2012, **22**, 14276.
9. X. Yang, X. Wang, Y. Feng, G. Zhang, T. Wang, W. Song, C. Shu, L. Jiang and C. Wang, *J. Mater. Chem. A*, 2013, **1**, 473-477.
10. R. Kumar, J. Rashid and M. A. Barakat, *RSC Advances*, 2014, **4**, 38334.
11. S. J. Tesh and T. B. Scott, *Adv Mater*, 2014, **26**, 6056-6068.
12. M. Khajeh, S. Laurent and K. Dastafkan, *Chem Rev*, 2013, **113**, 7728-7768.
13. R. Kumar, M. Ehsan and M. A. Barakat, *Journal of Industrial and Engineering Chemistry*, 2014, **20**, 4202-4206.
14. K. Yao, J. Gong, J. Zheng, L. Wang, H. Tan, G. Zhang, Y. Lin, H. Na, X. Chen, X. Wen and T. Tang, *The Journal of Physical Chemistry C*, 2013, **117**, 17016-17023.
15. W. Cai, Y. Hu, J. Yu, W. Wang, J. Zhou and M. Jaroniec, *RSC Adv.*, 2015, **5**, 7066-7073.
16. X. Sun and Y. Li, *Angewandte Chemie*, 2004, **116**, 607-611.
17. M. K. Naskar, *J. Am. Ceram. Soc.*, 2010, **93**, 1260–1263.
18. Y. L. Feng, W. C. Lu, L. M. Zhang, X. H. Bao, B. H. Yue, Y. Iv and X. F. Shang, *Cryst Growth Des*, 2008, **8**, 1426-1429.
19. J. Xiao, H. Ji, Z. Shen, W. Yang, C. Guo, S. Wang, X. Zhang, R. Fu and F. Ling, *RSC Advances*, 2014, **4**, 35077.
20. T. Kim, J. Lian, J. Ma, X. Duan, and W. Zheng, *Cryst Growth Des*,2010, **10**, 2928-2933.
21. X. Yu, J. Yu, B. Cheng, and M. Jaroniec,*J. Phys. Chem. C,*2009**, 113***,* 17527–17535.
22. W. Cai, J. Yu, B. Cheng, B. L. Su, and M. Jaroniec, *J. Phys. Chem. C,*2009**, 113***,* 14739–14746.
23. L. Wang, J. Li, Y. Wang, L. Zhao and Q. Jiang, *Chemical Engineering Journal*, 2012, **181-182**, 72-79.
24. R. Yang, Y. Wang, M. Li and Y. J. Hong, *Acs Sustain Chem Eng*, 2014, **2**, 1270-1279.
25. Z. Cui, H. Yin, Q.Nie, *JALLOY COMPD*,2015, **632,**402–407.

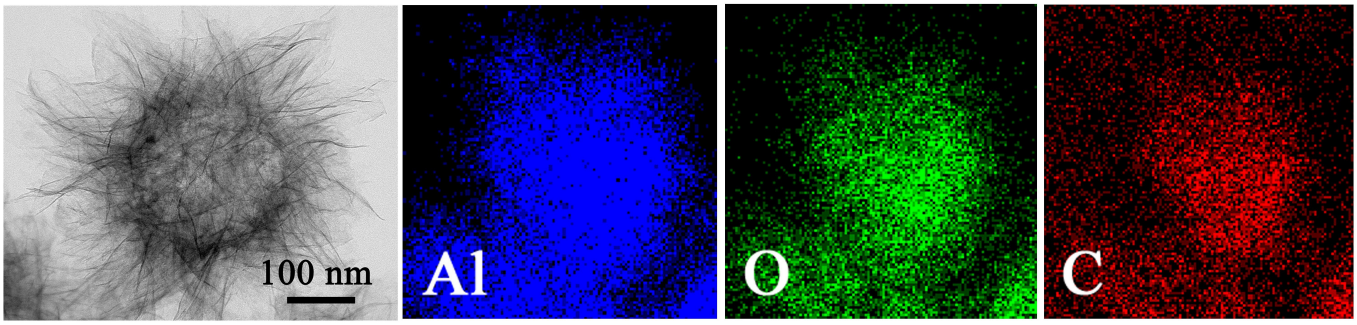

A single flower-like γ-Al_2O_3@C structures and the elemental mappings